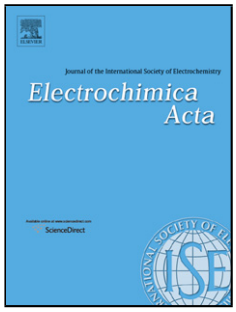

Title: Ultrathin Al_2O_3 Coatings for Improved Cycling Performance and Thermal Stability of $LiNi_{0.5}Co_{0.2}Mn_{0.3}O_2$ Cathode Material

Author: Yang Shi Minghao Zhang Danna Qian Ying Shirley Meng

PII: S0013-4686(16)30768-X
DOI: http://dx.doi.org/doi:10.1016/j.electacta.2016.03.185
Reference: EA 27015

To appear in: *Electrochimica Acta*

Received date: 5-1-2016
Revised date: 29-3-2016
Accepted date: 30-3-2016

Please cite this article as: Yang Shi, Minghao Zhang, Danna Qian, Ying Shirley Meng, Ultrathin Al2O3 Coatings for Improved Cycling Performance and Thermal Stability of LiNi0.5Co0.2Mn0.3O2 Cathode Material, Electrochimica Acta http://dx.doi.org/10.1016/j.electacta.2016.03.185

Ultrathin Al_2O_3 Coatings for Improved Cycling Performance and Thermal Stability of $LiNi_{0.5}Co_{0.2}Mn_{0.3}O_2$ Cathode Material

Yang Shi[1], Minghao Zhang[1,2], Danna Qian[2], Ying Shirley Meng[1,2,*]

1 Materials Science and Engineering, University of California San Diego, 9500 Gilman Drive, La Jolla, CA 92093, United States

2 Department of NanoEngineering, University of California San Diego, 9500 Gilman Drive, La Jolla, CA 92093, United States

Highlights

- Ultrathin Al_2O_3 coatings are deposited on $LiNi_{0.5}Co_{0.2}Mn_{0.3}O_2$ composite electrodes by Atomic Layer Deposition
- The Al_2O_3 coating effectively improves cycling performance in high voltage ranges
- The Al_2O_3 coating decreases charge transfer resistance and enhances Li ion diffusivity
- The Al_2O_3 coating increases thermal stability and delays exothermic reactions

Abstract

Ultrathin Al_2O_3 is directly deposited on $LiNi_{0.5}Co_{0.2}Mn_{0.3}O_2$ (NCM523) composite electrodes by atomic layer deposition (ALD). After 4 ALD cycles, the coated cathode exhibits significantly improved cycling performance and thermal stability, especially at high working voltage. The capacity retention of the coated cathode is 76.8% after 30 cycles in the voltage range of 2-4.8 V,

compared to 58.4% of pristine cathode. The exothermic peak in differential scanning calorimetry (DSC) analysis, corresponding to the reactions between delithiated electrode and electrolyte, is also delayed after cycling. The improvement is attributed to the reduced charge transfer resistance and enhanced Li ion diffusivity, as the Al_2O_3 coating may suppress the side reactions between electrode and electrolyte, and inhibit the oxygen release under high operating voltage.

Keywords

Lithium-ion battery; ALD coating; $LiNi_{0.5}Co_{0.2}Mn_{0.3}O_2$; high voltage cyclability; thermal stability.

1. Introduction

With the rapid development of electric vehicles (EVs), hybrid electric vehicles (HEVs), and plug-in hybrid electric vehicles (PHEVs), extensive study has been conducted on lithium-ion batteries with higher energy density and longer cycle life [1]. NCM type materials have attracted much interest due to their high energy density and relatively low cost [2]. Among many other materials, $LiNi_{0.5}Co_{0.2}Mn_{0.3}O_2$ (NCM523) is viewed as a promising candidate, especially while operating under high voltage. However, severe capacity degradation at high working voltage was reported [3, 4], associated with side reactions between electrodes and electrolyte [5]. Another critical issue is that NCM523 tends to be thermally unstable because of oxygen release when it is charged to a high voltage (above 4.6V) [5]. In order to mitigate these problems, surface modification has been investigated [6, 7].

Surface modification could be performed through conventional wet-chemical methods [6-13], however, the surface coverage, thickness, and uniformity of the coating layer cannot be controlled

precisely [14]. Moreover, these methods usually require post heat treatment and could not be applied on as-formed composite electrodes [15]. In contrast, atomic layer deposition (ALD) has a thickness control at the Angstrom or monolayer level [16]. It could be applied directly on as-formed electrodes so that the original electrical pathways constructed between the components in electrodes are not disrupted [15]. High surface coverage could be achieved by coating composite electrodes compared to coating raw material powder, since the direct coating on powder might be partly removed during grounding of active material, binder, and conductive carbon [17].

Al_2O_3 ALD coating was successfully applied on $LiCoO_2$ cathodes to improve their cycling performance [18, 19] and there were a few reports on Al_2O_3 ALD coatings on NCM type cathodes to increase their capacity retention [20, 21]. However, all of the above reports had a cut-off voltage of 4.5 V and there were few reports on the electrochemical performance of NCM type cathode working in the high voltage range (above 4.6 V) modified by Al_2O_3 ALD technique. In addition, the influence of ALD coating on thermal stability of cathode materials has never been studied in previous reports. Considering that the charged cathode releases oxygen at high temperature, combusts the electrolyte exothermally, and leads to thermal runaway in practical applications [22], it is critical to characterize the thermal stability of Al_2O_3 ALD coated electrodes at charged state.

In this study, an ultrathin coating of Al_2O_3 was deposited directly on the as-formed composite NCM523 electrodes. Electrochemical impedance spectroscopy (EIS) and differential scanning calorimetry (DSC) experiments have been applied to investigate the influence of Al_2O_3 ALD coating on the cycling performance and thermal stability of NCM523 electrodes.

2. Experimental

2.1 Electrode preparation

The composite electrode was composed of NCM5232 (TODA America, Inc (NCM 04ST)) powder, polyvinylidene fluoride (PVDF, Kynar 710), and carbon black (Timcal, Super C65) in weight ratio of 93:4:3. The three components were mixed to prepare the slurries in 1-Methyl-2-pyrrolidinone (NMP, anhydrous, 99.5%, Sigma Aldrich). Then the slurries were cast on Al-foil using a doctor blade and dried in vacuum at 80 °C for 24 h.

2.2 Deposition of Al_2O_3 coatings

Deposition of Al_2O_3 coatings on the as-formed composite electrode was carried out at 180 °C in an ALD system (Beneq TFS200), with trimethylaluminum (TMA) and water as the precursors, and N_2 as the carrier. A complete ALD cycle includes the following steps: (1) pulsing TMA for 200 ms, (2) purging the chamber with N_2 for 6 s at a flow rate of 300 sccm, (3) pulsing water for 50 ms, and (4) purging the chamber with N_2 for 6 s at a flow rate of 300 sccm. 2, 4, 8 and 15 ALD cycles were applied on electrode sheets, followed by drying in a vacuum at 120 °C for 12 h to remove residual surface reactants.

2.3 Characterization

The electrode materials were removed from the Al substrate and the crystal structure of the electrodes was examined by X-ray Powder Diffraction (XRD) employing Cu K_α radiation. The morphology and size distribution of the raw NCM523 particles were characterized by Scanning Electron Microscope (SEM) (Phillips XL30) and the images were shown in Supplementary **Fig. S1**. The morphology and thickness of the coating were examined by Transmission Electron

Microscopy (TEM) (FEI Tecnai G2 Sphera cryo-electron microscope). The chemical composition of the coating was analyzed by X-ray Photoelectron Spectroscopy (XPS) (Thermo ESCALAB 250Xi) with Al K_α radiation, and all the spectra were calibrated by assigning the C 1s peak at 284.8 eV. The atomic signals on the surface of the electrodes were measured by Oxford Energy Dispersive X-ray Spectroscopy (EDS) attachment of Phillips XL30 SEM.

2.4 Electrochemical measurements

Disc electrodes were punched out, compressed by passing through a rolling mill and dried in vacuum oven for 4 h before placing them into an Ar-filled glovebox (H_2O < 0.1 ppm). The active mass loading was about 2.5 mg/cm^2. 2016 coin cells were assembled with Li metal disc (1.1 mm) as anode, 1 M $LiPF_6$ in ethylene carbonate and diethyl methyl carbonate (EC: DMC 3:7 wt) as electrolyte, and trilayer PP/PE/PP films (2320, Celgard Inc.) as a separator.

The coin cells were allowed to rest for 2 h before the electrochemical tests were performed. Galvanostatic charge-discharge was carried out using an Arbin BT2000 battery testing system. The cells were initially charged and discharged at C/10 (1C = 200 mA g^{-1}) for one cycle, followed by cycling at 1C in the potential range of 2-4.8 V and 3-4.6 V. The electrochemical impedance spectroscopy (EIS) tests were carried out at discharged state in the frequency range of 10^6 Hz to 10^{-2} Hz with signal amplitude of 5 mV by Solartron Impedance/Gain-Phase Analyzer.

2.5 DSC analysis

The coin cells were charged in different conditions and the cathode material at charged state was removed from the Al substrate. A stainless-steel pan was filled with 2 mg cathode material and 5 μL electrolyte, and then sealed with a gold-plated copper seal (which can withstand 150 atm of

pressure before rupturing). DSC measurements were performed on the sealed pans in a DSC 8000 (Perkin Elmer) using a temperature scan rate of 1 °C/min. At least three measurements were carried out for each data point to ensure reproducibility.

3. Results and Discussion

XRD patterns of the pristine and Al_2O_3 coated electrodes with 4 ALD cycles are shown in **Fig. 1**. A typical pattern of α-$NaFeO_2$ structure with R $\overline{3}$ m space group is observed for both electrodes. As expected, the Al_2O_3 coating has no influence on the crystal structure of the substrate material. No extra peak was detected in the XRD patterns, which could be ascribed to the amorphous Al_2O_3.

Fig. 2(a) and **(b)** show the HRTEM images of the pristine and 15 ALD cycles coated electrode materials. 15 ALD cycles were applied on the electrode to get a thicker layer of Al_2O_3 for TEM observation, since the Al_2O_3 coating grows linearly with ALD cycles. More than 20 particles were examined and **Fig. 2** demonstrates the clear image of the representative particle. The lattice fringe of pristine NCM523 cathode (**Fig. 2(a)**) displays its well-ordered layered structure, and the Al_2O_3 coated cathode (**Fig. 2(b)**) exhibits a uniform amorphous outer layer on the surface with a thickness of ~1.65 nm. The average growth rate is ~0.11 nm per cycle, which is consistent with previous reports of 0.11-0.12 nm per cycle [23]. **Fig. 3** shows the XPS images of the pristine and 4 ALD cycles coated electrodes. The binding energy of 74.7 eV in the XPS spectra could be attributed to Al 2p, which is assigned to Al-O chemical bond of Al_2O_3 [19]. The existence of an Al_2O_3 coating on the electrode is confirmed, while Al element is not detected on the pristine electrode. The EDS images of the pristine and 4 ALD cycles coated electrodes are shown in **Fig. S2** to further confirm

the existence of the Al_2O_3 coating.

The present research is focused on the Al_2O_3 coated cathode with 4 ALD cycles, which exhibits the best cycling performance among all the coated cathodes with different ALD cycles (see Supplementary **Fig. S2**). To acquire high capacity, the cathodes should be operated under a broad voltage range, therefore an extreme condition with the working voltage range of 2-4.8 V was designed to investigate the capacity retention. A narrower working voltage range of 3-4.6 V, which is a conventional high voltage condition, was selected as a comparison to study the influence of Al_2O_3 ALD coating on the capacity retention in different voltage ranges. **Fig. 4** shows the cycling performance of pristine and Al_2O_3 coated NCM523 cathode in the voltage range of 2-4.8 V and 3-4.6 V at 1C after the initial cycle at C/10, and the inset picture displays the coulombic efficiency of each cycle. In both voltage ranges, the Al_2O_3 coated cathode exhibits improved cycling stability compared to the pristine cathode. The capacity retention of Al_2O_3 coated cathode is 76.8% after 30 cycles in the high voltage range (2-4.8 V) while that of pristine cathode is only 58.4%. In the low voltage range (3-4.6 V), the coated cathode could still exhibit a capacity retention of 75.5% even after 100 cycles while the pristine cathode has merely 59.9% capacity retention. A similar degree of improvement with the Al_2O_3 ALD coating is achieved for both voltage ranges. It takes 100 cycles to achieve the desired result in the low voltage range, while only 30 cycles are enough for the high voltage range, which indicates that the Al_2O_3 ALD coating has more obvious enhancement in capacity retention in the higher voltage range. The slightly decreased capacity during the first few cycles of the coated sample could be ascribed to the lack of electronic conductivity of the Al_2O_3 coatings, and it is compensated due to the improved capacity retention effect of Al_2O_3

coatings in the following cycles. The initial coulombic efficiency of the Al_2O_3 coated cathode is also higher than that of the pristine cathode in both voltage ranges of 2-4.8 V and 3-4.6 V (see **Table 1**). **Fig. 5** shows the voltage versus capacity profiles of each charge-discharge cycle in the voltage range of 2-4.8 V and 3-4.6 V for the pristine and Al_2O_3 coated cathode. In each cycle, there is a voltage drop at the beginning of discharging. The pristine cathode has larger voltage drops than Al_2O_3 coated cathode while working in both voltage ranges. The voltage drop of pristine cathode is 0.81 V after 30 cycles in the voltage range of 2-4.8 V while that of coated cathode is 0.47 V (see **Table 2**).

It is notable that the side reactions between electrode and electrolyte causes capacity degradation for layered cathode [6]. Impurities such as Li_2O could accelerate the decomposition of $LiPF_6$, releasing harmful HF and inactive LiF phase [24]. These side reactions could increase the charge transfer resistance [25] and the LiF phase formed on the electrode surface is highly resistive to Li-ion migration [26], which results in a capacity and voltage fading. Such side reactions can be accelerated under a higher voltage range of 2-4.8 V [6]. The Al_2O_3 ALD coating is supposed to prevent the direct contact between electrode material and electrolyte, and suppress the side reactions in order to improve the cycling stability [27, 28]. The Al_2O_3 ALD coating has more obvious enhancement in capacity retention in the voltage range of 2-4.8 V than 3-4.6 V due to the more severe side reactions under a higher voltage range. The lower initial coulombic efficiency of pristine cathode than coated cathode, resulted from the longer charging time, indicates that more side reactions happened between pristine cathode and electrolyte. The larger voltage drop of the pristine cathode than coated cathode also signifies severe polarization caused by side reactions [29,

30]. **Fig. 6** compares the dQ/dV plots of the pristine and coated cathodes, which were obtained by differential analysis of the charge and discharge curves. The redox peaks correspond to the plateaus in the charge and discharge curves. For the pristine cathodes, the oxidation peak shifts to higher voltage and the reduction peak shifts to lower voltage after cycles. On the contrary, the coated cathodes show much smaller redox peaks shift. This further proves that the pristine cathodes have more severe polarization compared to the coated cathodes.

To further explore the effects of Al_2O_3 ALD coating on NCM523 cathode and the factors for enhanced cyclability, EIS measurements were performed on the cells prepared with pristine or Al_2O_3 coated cathode at discharged state. **Fig. 6** shows Nyquist plots of the pristine and Al_2O_3 coated cathode cycled in different voltage ranges, and the inset picture displays the plots at an enlarged scale. The corresponding equivalent circuit was used to fit the Nyquist plots and get quantitative value of resistance. R_s is the electrolyte resistance at high frequency. R_{sei} at middle frequency, and R_{ct} at low frequency demonstrate the resistances of the solid electrolyte interface (SEI) and the charge-transfer resistance, respectively. W is the Warburg impedance related to the diffusion of lithium ions [31]. **Table 3** shows the resistance value according to the fitting results from the equivalent circuit and the cell potentials in EIS measurements. Compared to the pristine cathode, a slightly increased R_{sei} value of the Al_2O_3 coated cathode is observed, indicating that the transport of Li^+ ions might be slightly impeded by the insulating ceramic Al_2O_3 layer. However, the value of R_{ct} for the pristine cathode increases to 219.4 Ω after 20 cycles in the voltage range of 2-4.8V, while the value of R_{ct} for Al_2O_3 coated cathode is only 60.8 Ω. The same trend is also observed in the low voltage range of 3-4.6V. The reason for the relatively lower R_{ct} value for the

coated cathode is that the Al_2O_3 coating prevents the direct contact between the cathode and electrolyte, and therefore suppresses side reactions. As mentioned earlier, the side reactions deteriorate at high working voltage, which is supported by the fact that the R_{ct} value in the voltage range of 2-4.8 V is higher than that in the voltage range of 3-4.6 V after 50 cycles. It is noticed that the value of R_{sei} for both pristine and Al_2O_3 coated cathode decrease over each cycle, which could be ascribed to the activation of the material in the initial several cycles and the gradual formation of ion conductive SEI layer. This trend is in agreement with the previous work of Shi et al. [32] and Xia et al. [33]. Some previous reports observed the increase of R_{sei} with cycles due to the thickening of SEI layer [10, 24]. It is possible that the SEI layers in our cycling tests were still in the activation process and the R_{sei} value might increase again (after 50 cycles for 2-4.8 V and 100 cycles for 3-4.6 V), which will be investigated in our future research.

The linear part of EIS in the low frequency is directly related to Li^+ diffusion in electrode and Li^+ diffusion coefficient could be calculated using the following equation [31].

$$D = \frac{R^2T^2}{2A^2n^4F^4C^2\sigma^2}$$

R is the gas constant, T is the absolute temperature, A is the surface area of the electrode, which is estimated based on the BET area (0.15 $m^2\ g^{-1}$ for NCM523 powders), n is the number of electrons involved in reaction (n=1), F is the Faraday constant, C is the concentration of Li^+ in the electrode (= ρ/M) based on the molecular weight of NCM523 (M) and density (ρ), and σ is the Warburg factor. The Warburg factor can be obtained from the slope of Z' vs. $\omega^{-1/2}$ plots (ω is the angular frequency) in the Warburg region [34]. The results of the Z' vs. $\omega^{-1/2}$ for the pristine and

Al_2O_3 coated cathode after 20 cycles in the voltage range of 2-4.8 V, along with the linear fitting curves, are shown in **Fig. 6 (f)**. The slope σ can be obtained and D can be calculated from the plot. The apparent diffusion coefficients for the pristine and Al_2O_3 coated cathode are 5.21×10^{-10} cm^2 s^{-1} and 4.98×10^{-9} cm^2 s^{-1}, respectively. The larger apparent Li^+ diffusion coefficient for Al_2O_3 coated cathode indicates that the Al_2O_3 layer facilitates the diffusion of Li^+ at the interface between electrode and electrolyte. There exists an energetically most favorable composition of lithiated Al_2O_3 ($Li_xAl_2O_3$) and the Li^+ in the optimal concentration in $Li_xAl_2O_3$ diffuses faster by four orders of magnitude than the Li^+ in a dilute concentration [35]. Since the optimal concentration is related to the thickness of the Al_2O_3 coating, it is possible that the ultrathin layer of Al_2O_3 might favor the Li^+ diffusion. The reduced charge transfer resistance and enhanced Li^+ diffusivity are the two main reasons for the improved cycling performance for Al_2O_3 coated electrodes.

ALD coating not only enhances the cycling performance of cathode material, but also influences its thermal stability. It is important to investigate the thermal interactions between the electrodes and electrolyte since thermal analysis in the presence of electrolyte better mimics the real battery behavior, and the experimental results were consistent with nail penetration tests on pouch cells [36, 37]. DSC measurements were carried out for the charged pristine and Al_2O_3 coated cathode to study the effects of A_2O_3 ALD coating on the thermal stability of NCM523 electrode in the presence of electrolyte. From the electrochemical characterization results above, the Al_2O_3 ALD coating has more obvious improvement in cycling stability in the voltage range of 2-4.8 V than 3-4.6 V, therefore the DSC measurements were carried out only on the cathodes charged to 4.8V. **Fig. 7(a)** shows the DSC curve of the cathode material after the cells were charged to 4.8 V. There is

no difference in peak temperature and the generated heat for the pristine and Al_2O_3 coated electrodes after the first charging. The exothermic peak temperature is 375 °C and the total generated heat is ~2700 J g^{-1}. The exothermic peak corresponds to the reaction between the electrolyte and charged cathode material, i.e. the oxidation of solvents by oxygen released from the cathode material [37]. **Fig. 7(b)** displays the DSC curves of cathode material charged to 4.8 V after the 20th cycle. The intensity of heat flow increased slightly for both electrodes due to the gradually decreased stability of cathode after cycling. The exothermic peaks are at 355 °C and 367 °C for the pristine and Al_2O_3 coated electrodes, respectively. The total generated heat increases from ~2700 J g^{-1} to ~3600 J g^{-1} for both the pristine and Al_2O_3 coated electrodes, indicating a decreased thermal stability after 20 cycles. Even though the generated heat remains the same, the exothermal peak temperature corresponding to the reaction between the electrolyte and charged cathode for the Al_2O_3 coated samples is delayed by 12 °C compared to the pristine samples, indicating a better thermal stability of the Al_2O_3 coated electrodes. At the first cycle, the charged cathode is quite stable, therefore the effect of Al_2O_3 coating is negligible. With decreasing structural stability upon cycles, the delay of exothermal peak due to the Al_2O_3 coating was observed. The coating suppresses the oxygen released by the decomposition of charged cathode, therefore delays the oxidation of electrolyte solvents. The endothermic peak in **Fig. 7 (a) (b)** around 225 °C might be the decomposition of $LiPF_6$ salt and the different shape of the endothermic peak in **Fig. 7 (b)** compared to **(a)** might come from the side reactions accumulated during high cut-off voltage cycling [38-40].

4. Conclusions

Ultrathin Al_2O_3 films is deposited using ALD on NCM523 composite electrodes. A significantly improved performance under high operating voltage associated with the Al_2O_3 ALD coating is demonstrated not only in cycle retention and coulombic efficiency, but also in thermal stability. The capacity retention of Al_2O_3 coated cathode is considerably better than that of pristine cathode in the voltage range of 2-4.8 V. The exothermic peak corresponding to the reaction between the charged electrode and electrolyte is delayed by 12 °C due to the existence of the Al_2O_3 ALD coating. The electrochemical analysis using EIS demonstrates the Al_2O_3 ALD coating suppresses side reactions between electrode and electrolyte, which reduces charge transfer resistance and enhances the apparent Li^+ diffusivity of the composite cathode. In addition, the thermal analyses using DSC demonstrates that oxygen release is inhibited to some extent so that thermal stability is improved after cycling.

Acknowledgements

This research is supported by Advanced Research Projects Agency - Energy (ARPA-E) under Grant No. DE-AR0000396. The authors are sincerely grateful to Professor Yu Qiao for the DSC equipment and suggestions on the manuscript writing.

References

[1] K. Yang, L.Z. Fan, J. Guo, X. Qu, Significant improvement of electrochemical properties of AlF_3-coated $LiNi_{0.5}Co_{0.2}Mn_{0.3}O_2$ cathode materials, Electrochim. Acta 63 (2012) 363.

[2] L. Peng, Y. Zhu, U. Khakoo, D. Chen, G. Yu, Self-assembled $LiNi_{1/3}Co_{1/3}Mn_{1/3}O_2$ nanosheet cathodes with tunable rate capability, Nano Energy, 17 (2015) 36.

[3] D. Wang, X. Li, Z. Wang, H. Guo, Y. Xu, Y. Fan, J. Ru, Role of zirconium dopant on the structure and high voltage electrochemical performances of $LiNi_{0.5}Co_{0.2}Mn_{0.3}O_2$ cathode materials for lithium ion batteries, Electrochim. Acta, 188 (2016) 48-56.

[4] D. Wang, X. Li, Z. Wang, H. Guo, Y. Xu, Y. Fan, Co-modification of $LiNi_{0.5}Co_{0.2}Mn_{0.3}O_2$ cathode materials with zirconium substitution and surface polypyrrole coating: towards superior high voltage electrochemical performances for lithium ion batteries, Electrochim. Acta, 196 (2016) 101-109.

[5] S.K. Jung, H. Gwon, J. Hong, K.Y. Park, D.H. Seo, H. Kim, J. Hyun, W. Yang, K. Kang, Understanding the degradation mechanisms of $LiNi_{0.5}Co_{0.2}Mn_{0.3}O_2$ cathode material in lithium ion batteries, Adv. Energy Mater., 4 (2014) 7.

[6] X.H. Liu, L.Q. Kou, T. Shi, K. Liu, L. Chen, Excellent high rate capability and high voltage cycling stability of Y_2O_3-coated $LiNi_{0.5}Co_{0.2}Mn_{0.3}O_2$, J. Power Sources 267 (2014) 874.

[7] Y.S. Lee, D. Ahn, Y.H. Cho, T.E. Hong, J. Cho, Improved rate capability and thermal stability of $LiNi_{0.5}Co_{0.2}Mn_{0.3}O_2$ cathode materials via nanoscale SiP_2O_7 coating, J. Electrochem. Soc. 158 (2011) A1354.

[8] W. Liu, M. Wang, X.L. Gao, W. Zhang, J. Chen, H. Zhou, X. Zhang, Improvement of the high-

temperature, high-voltage cycling performance of $LiNi_{0.5}Co_{0.2}Mn_{0.3}O_2$ cathode with TiO_2 coating, J. Alloys Compd. 543 (2012) 181.

[9] K.J. Cao, L. Wang, L.C. Li, G.C. Liang, Effects of Al_2O_3 coating on the structural and electrochemical performance of $LiNi_{0.5}Co_{0.2}Mn_{0.3}O_2$ cathode material, in: China Functional Materials Technology and Industry Forum, Applied Mechanics and Materials, Vol. 320, Trans Tech Publications Ltd, Stafa-Zurich, 2013, p. 235.

[10] F. Wu, J. Tian, Y. Su, Y. Guan, Y. Jin, Z. Wang, T. He, L. Bao, S. Chen, Lithium-active molybdenum trioxide coated $LiNi_{0.5}Co_{0.2}Mn_{0.3}O_2$ cathode material with enhanced electrochemical properties for lithium-ion batteries, J. Power Sources 269 (2014) 747.

[11] Y. Bai, X. Wang, S. Yang, X. Zhang, X. Yang, H. Shu, Q. Wu, The effects of $FePO_4$-coating on high-voltage cycling stability and rate capability of $Li[Ni_{0.5}Co_{0.2}Mn_{0.3}]O_2$, J. Alloys Compd. 541 (2012) 125.

[12] Y. Huang, F.M. Jin, F.J. Chen, L. Chen, Improved cycle stability and high-rate capability of Li_3VO_4-coated $Li[Ni_{0.5}Co_{0.2}Mn_{0.3}]O_2$ cathode material under different voltages, J. Power Sources 256 (2014) 1.

[13] D. Wang, X. Li, W. Wang, Z. Wang, H. Guo, J. Ru, Improvement of high voltage electrochemical performance of $LiNi_{0.5}Co_{0.2}Mn_{0.3}O_2$ cathode materials via Li_2ZrO_3 coating, Ceram. Int. 41 (2015) 6663.

[14] I.D. Scott, Y.S. Jung, A.S. Cavanagh, Y. Yan, A.C. Dillon, S.M. George, S.H. Lee, Ultrathin coatings on nano-$LiCoO_2$ for li-ion vehicular applications, Nano Lett. 11 (2011) 414.

[15] Y.S. Jung, A.S. Cavanagh, L.A. Riley, S.H. Kang, A.C. Dillon, M.D. Groner, S.M. George,

S.H. Lee, Ultrathin direct atomic layer deposition on composite electrodes for highly durable and safe li-ion batteries, Adv. Mater. 22 (2010) 2172.

[16] S.M. George, Atomic layer deposition: an overview, Chem. Rev. 110 (2010) 111.

[17] Y. S. Jung, A.S. Cavanagh, Y. Yan, S.M. George, A. Manthiram, Effects of atomic layer deposition of Al_2O_3 on the $Li[Li_{0.20}Mn_{0.54}Ni_{0.13}Co_{0.13}]O_2$ cathode for lithium-ion batteries, J. Electrochem. Soc. 158 (2011) A1298.

[18] Y.S. Jung, A.S. Cavanagh, A.C. Dillon, M.D. Groner, S.M. George, S.H. Lee, Enhanced stability of $LiCoO_2$ cathodes in lithium-ion batteries using surface modification by atomic layer deposition, J. Electrochem. Soc. 157 (2010) A75.

[19] H.M. Cheng, F.M. Wang, J.P. Chu, R. Santhanam, J. Rick, S.C. Lo, Enhanced cycleabity in lithium ion batteries: resulting from atomic layer deposition of Al_2O_3 or TiO_2 on $LiCoO_2$ electrodes, J. Phys. Chem. C 116 (2012) 7629.

[20] L.A. Riley, S. Van Atta, A.S. Cavanagh, Y. Yan, S.M. George, P. Liu, A.C. Dillon, S.H. Lee, Electrochemical effects of ALD surface modification on combustion synthesized $LiNi_{1/3}Mn_{1/3}Co_{1/3}O_2$ as a layered-cathode material, J. Power Sources, 196 (2011) 3317.

[21] J.W. Kim, J.J. Travis, E. Hu, K.W. Nam, S.C. Kim, C.S. Kang, J.H. Woo, X.Q. Yang, S.M. George, K.H. Oh, S.J. Cho, S.H. Lee, Unexpected high power performance of atomic layer deposition coated $Li[Ni_{1/3}Mn_{1/3}Co_{1/3}]O_2$ cathodes, J. Power Sources 254 (2014) 190.

[22] D.D. MacNeil, J.R. Dahn, Can an electrolyte for lithium-ion batteries be too stable?, J. Electrochem. Soc. 150 (2003) A21.

[23] J.W. Kim, D.H. Kim, D.Y. Oh, H. Lee, J.H. Kim, J.H. Lee, Y.S. Jung, Surface chemistry of

$LiNi_{0.5}Mn_{1.5}O_4$ particles coated by Al_2O_3 using atomic layer deposition for lithium-ion batteries, J. Power Sources 274 (2015) 1254.

[24] L. Li, Z. Chen, Q. Zhang, M. Xu, X. Zhou, H. Zhu, K. Zhang, A hydrolysis-hydrothermal route for the synthesis of ultrathin $LiAlO_2$-inlaid $LiNi_{0.5}Co_{0.2}Mn_{0.3}O_2$ as a high-performance cathode material for lithium ion batteries, J. Mater. Chem. A 3 (2015) 894.

[25] X. Xiong, D. Ding, Y. Bu, Z. Wang, B. Huang, H. Guo, X. Li, Enhanced electrochemical properties of a $LiNiO_2$-based cathode material by removing lithium residues with $(NH_4)_2HPO_4$, J. Mater. Chem. A 2 (2014) 11691.

[26] J.S. Gnanaraj, E. Zinigrad, M.D. Levi, D. Aurbach, M. Schmidt, A comparison among $LiPF_6$, $LiPF_3(CF_2CF_3)_3$ (LiFAP), and $LiN(SO_2CF_2CF_3)_2$ (LiBETI) solutions: electrochemical and thermal studies, J. Power Sources 119-121 (2003) 799.

[27] L.J. Fu, H. Liu, C. Li, Y.P. Wu, E. Rahm, R. Holze, H.Q. Wu, Surface modifications of electrode materials for lithium ion batteries, Solid State Sci. 8 (2006) 113.

[28] J. Cho, Y.J. Kim, B. Park, $LiCoO_2$ cathode material that does not show a phase transition from hexagonal to monoclinic phase, J. Electrochem. Soc. 148 (2001) A1110.

[29] J. Shim, R. Kostecki, T. Richardson, X. Song, K.A. Striebel, Electrochemical analysis for cycle performance and capacity fading of a lithium-ion battery cycled at elevated temperature, J. Power Sources 112 (2002) 222.

[30] R. Jorn, R. Kumar, D.P. Abraham, G.A. Voth, Atomistic modeling of the electrode-electrolyte interface in li-ion energy storage systems: electrolyte structuring, J. Phys. Chem. C 117 (2013) 3747.

[31] J. Ni, H. Zhou, J. Chen, X. Zhang, Improved electrochemical performance of layered $LiNi_{0.4}Co_{0.2}Mn_{0.4}O_2$ via Li_2ZrO_3 coating, Electrochim. Acta 53 (2008) 3075.

[32] S.J. Shi, J.P. Tu, Y.Y. Tang, X.Y. Liu, Y.Q. Zhang, X.L. Wang, C.D. Gu, Enhanced cycling stability of $Li[Li_{0.2}Mn_{0.54}Ni_{0.13}Co_{0.13}]O_2$ by surface modification of MgO with melting impregnation method, Electrochim. Acta 88 (2013) 671.

[33] L. Xia, K. Qiu, Y. Gao, X. He, F. Zhou, High potential performance of Cerium-doped $LiNi_{0.5}Co_{0.2}Mn_{0.3}O_2$ cathode material for li-ion battery, J. Mater. Sci. 50 (2015) 2914.

[34] S. Yang, X. Wang, X. Yang, Y. Bai, Z. Liu, H. Shu, Q. Wei, Determination of the chemical diffusion coefficient of lithium ions in spherical $Li[Ni_{0.5}Mn0.3Co_{0.2}]O_2$, Electrochim. Acta 66 (2012) 88.

[35] S.C. Jung, Y.K. Han, How Do Li Atoms Pass through the Al_2O_3 Coating Layer during Lithiation in Li-ion Batteries?, J. Phys. Chem. Lett., 4 (2013) 2681.

[36] S.K. Martha, O. Haik, E. Zinigrad, I. Exnar, T. Drezen, J.H. Miners, D. Aurbach, On the thermal stability of olivine cathode materials for lithium-ion batteries, J. Electrochem. Soc. 158 (2011) A1115.

[37] Y.K. Sun, S.T. Myung, B.C. Park, J. Prakash, I. Belharouak, K. Amine, High-energy cathode material for long-life and safe lithium batteries, Nat. Mater. 8 (2009) 320.

[38] G.G. Botte, R.E. White, Z.M. Zhang, Thermal stability of $LiPF_6$-EC : EMC electrolyte for lithium ion batteries, J. Power Sources 97-8 (2001) 570.

[39] K.S. Gavritchev, G.A. Sharpataya, A.A. Smagin, E.N. Malyi, V.A. Matyukha, Calorimetric study of thermal decomposition of lithium hexafluorophosphate, J. Therm. Anal. Calorim. 73

(2003) 71.

[40] E. Zinigrad, L. Larush-Asraf, J.S. Gnanaraj, M. Sprecher, D. Aurbach, On the thermal stability of $LiPF_6$, Thermochim. Acta 438 (2005) 184.

Figures

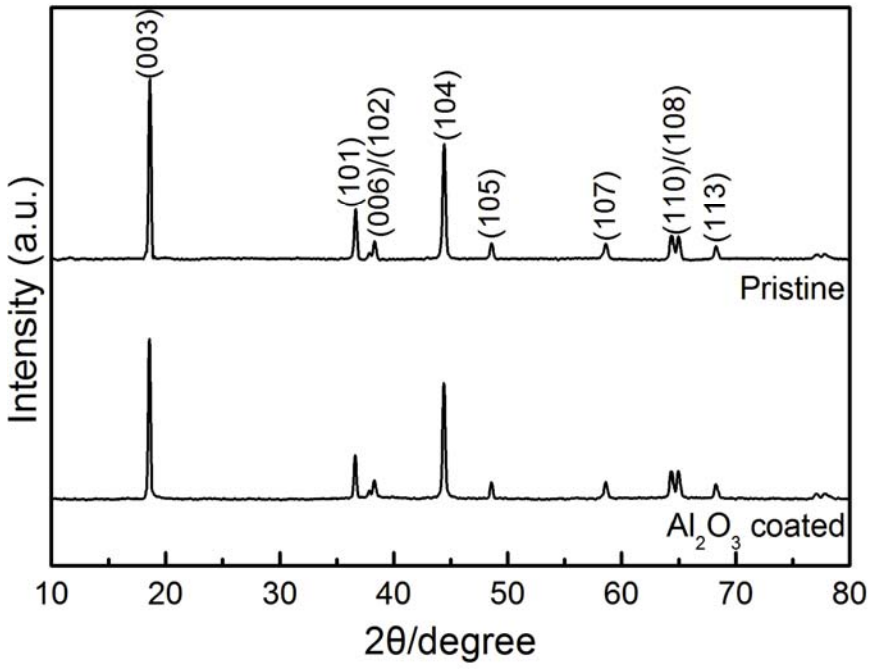

Fig. 1 XRD patterns of pristine and Al_2O_3 coated NCM523 electrodes

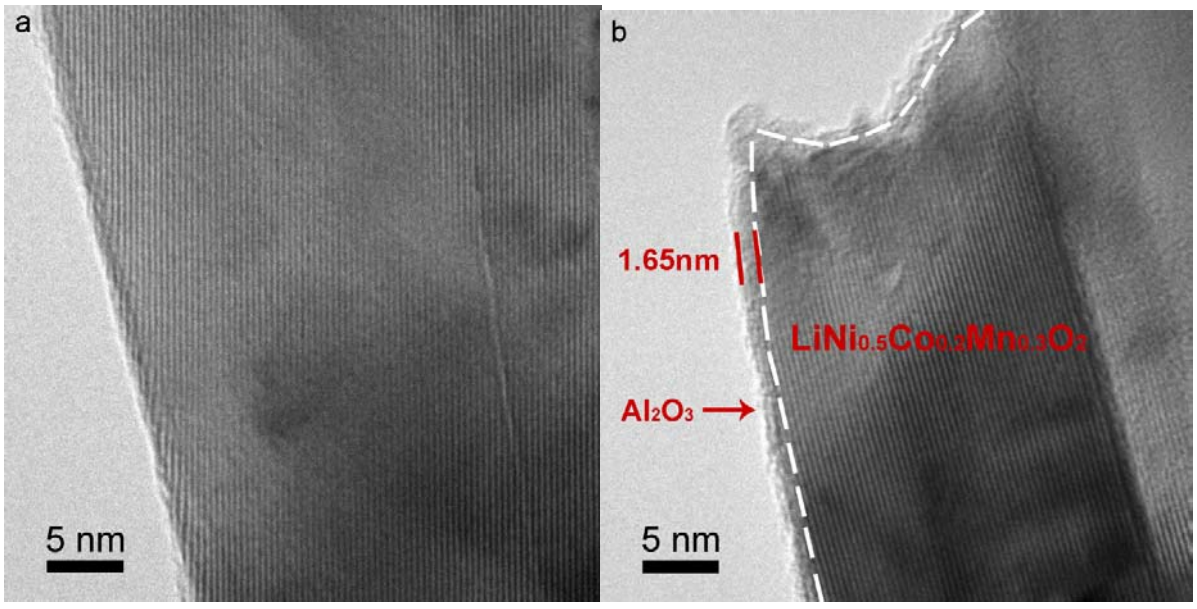

Fig. 2 HRTEM images of NCM523 particles before **(a)** and after **(b)** Al_2O_3 ALD coatings

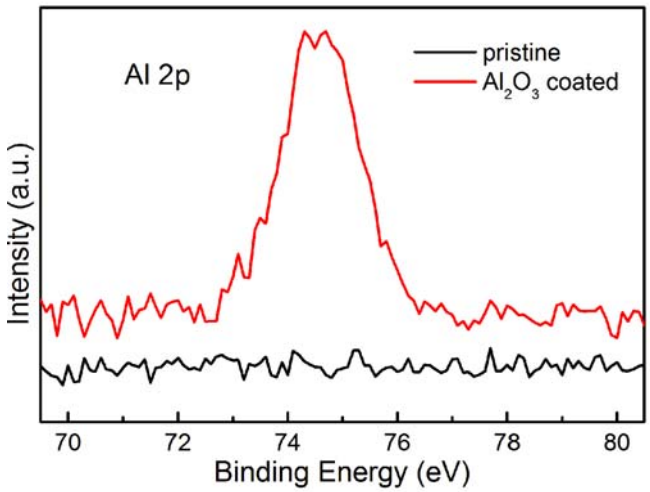

Fig. 3 XPS spectrum of Al 2p for pristine and Al_2O_3 coated electrode

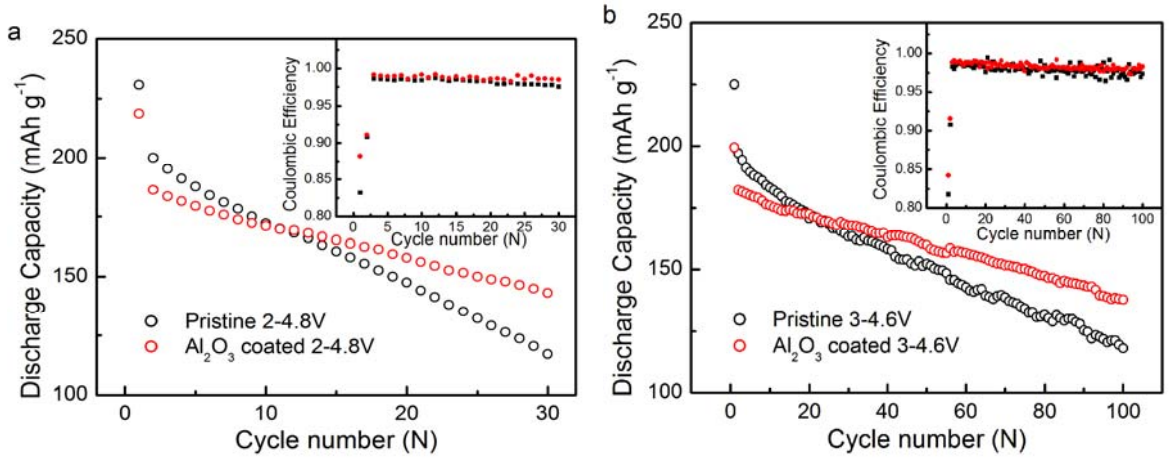

Fig. 4 Cycling performance of pristine and Al_2O_3 coated electrodes at 1C (a) 2-4.8 V and (b) 3-4.6 V after the initial cycle at C/10

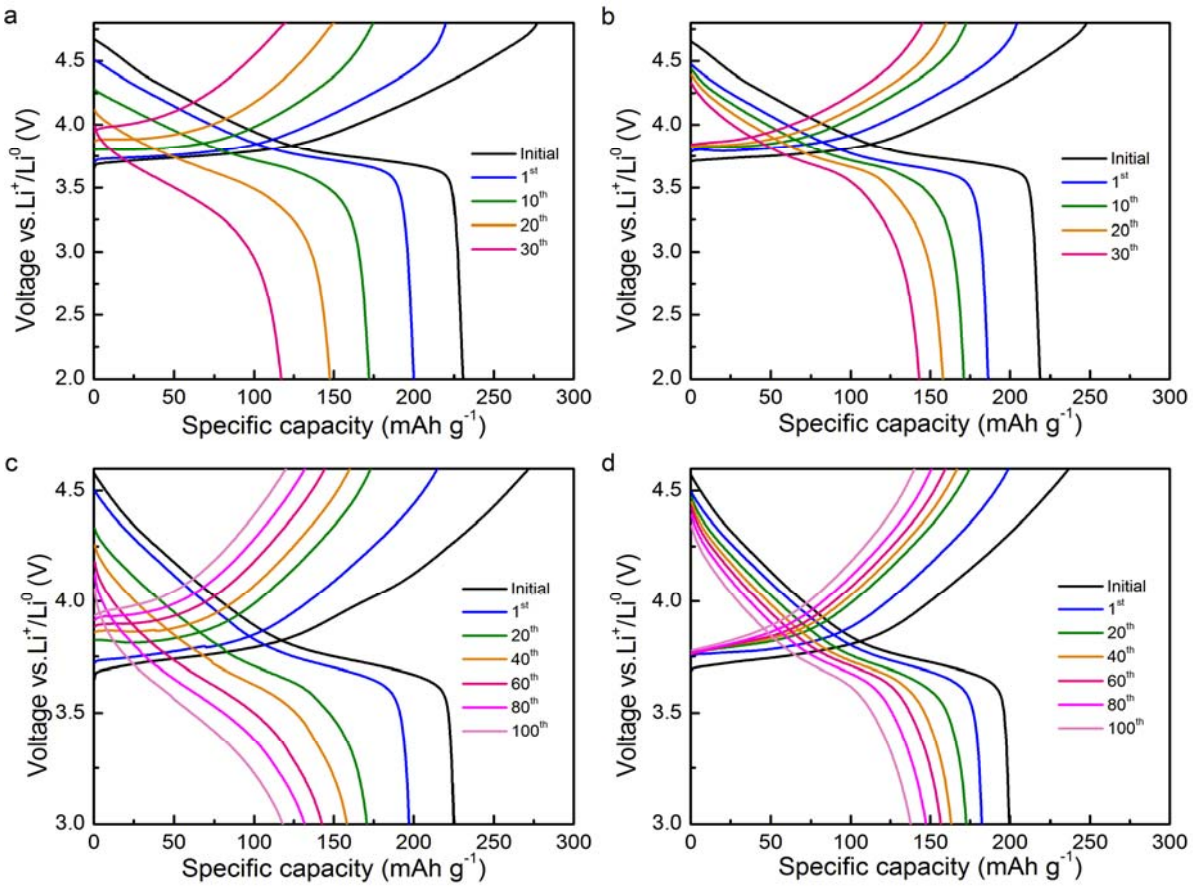

Fig. 5 Voltage versus capacity profiles of electrodes cycled at 1C after the initial cycle at C/10 (a) pristine 2-4.8 V, (b) Al_2O_3 coated 2-4.8 V, (c) pristine 3-4.6 V, and (d) Al_2O_3 coated 3-4.6 V

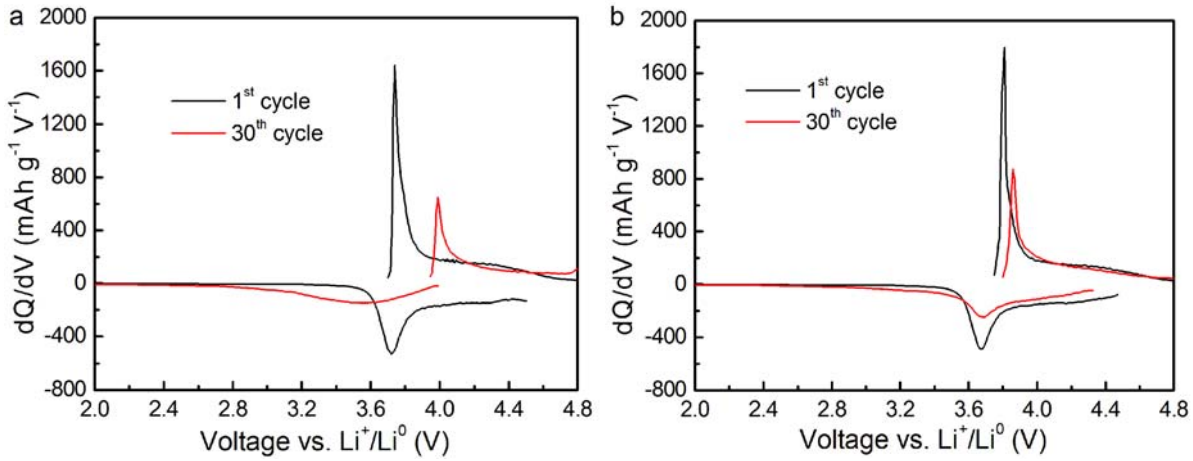

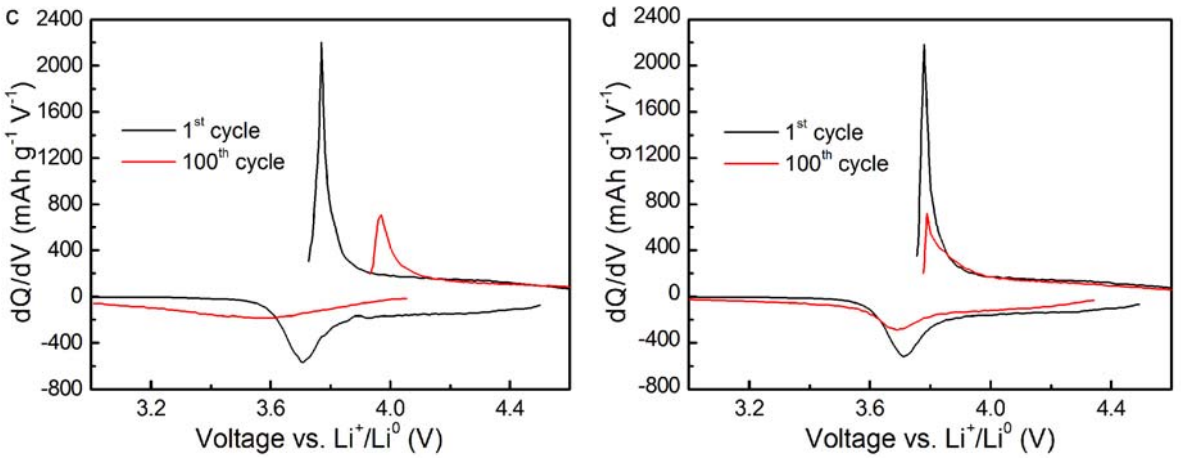

Fig. 6 Differential capacity dQ/dV versus voltage profiles of electrodes (a) pristine 2-4.8 V, (b) Al_2O_3 coated 2-4.8 V, (c) pristine 3-4.6 V, and (d) Al_2O_3 coated 3-4.6 V

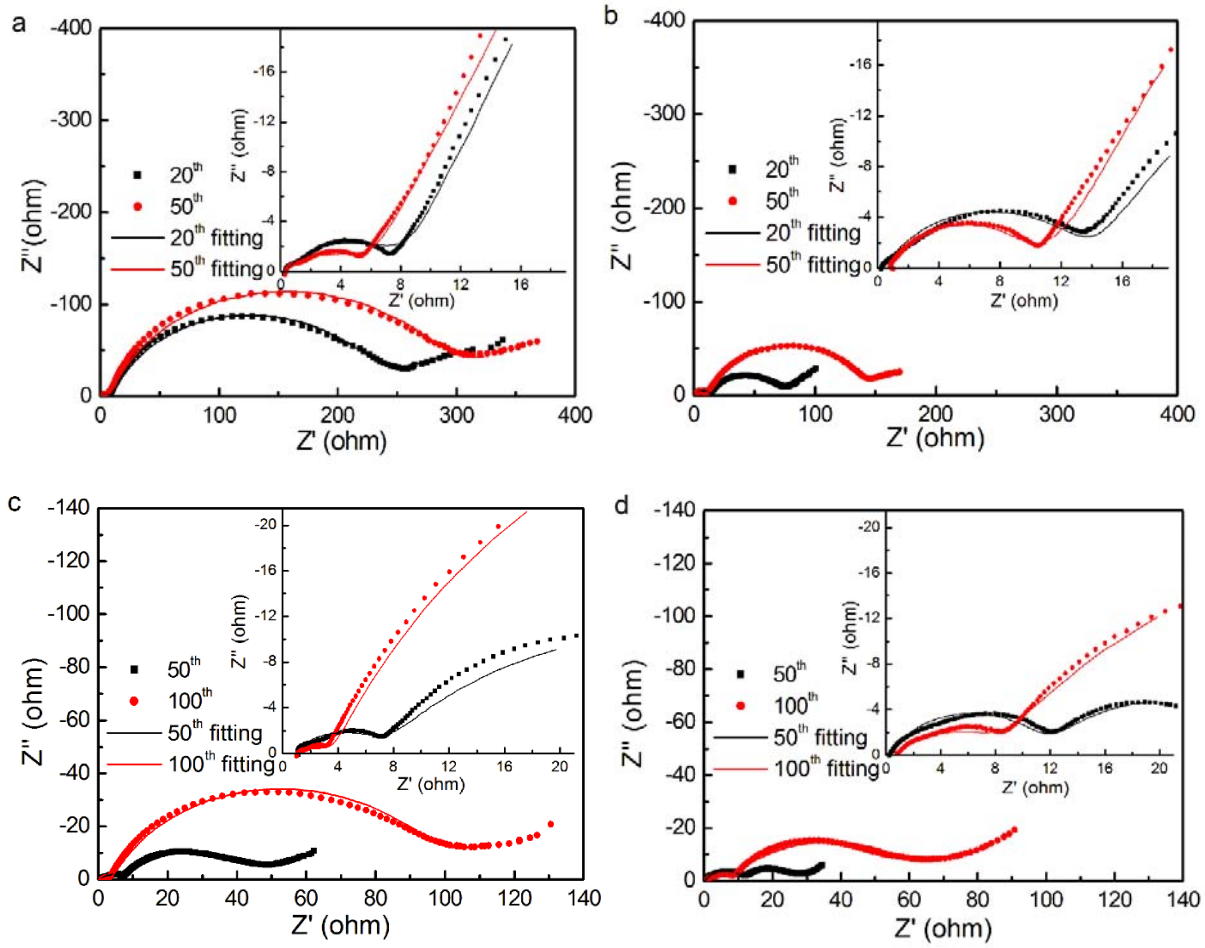

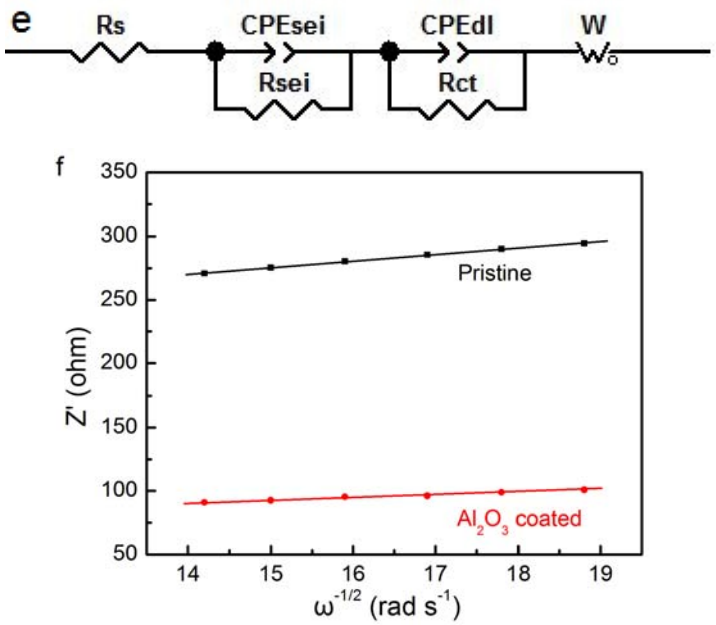

Fig. 7 Nyquist plots and fitting plots of pristine and Al_2O_3 coated electrodes after cycling at 1C **(a)** pristine 2-4.8 V, **(b)** Al_2O_3 coated 2-4.8 V, **(c)** pristine 3-4.6 V, **(d)** Al_2O_3 coated 3-4.6 V, **(e)** Equivalent circuit to fit Nyquist plots, and **(f)** Relationship between real parts of the complex impedance and $\omega^{-1/2}$ for pristine and Al_2O_3 coated electrodes

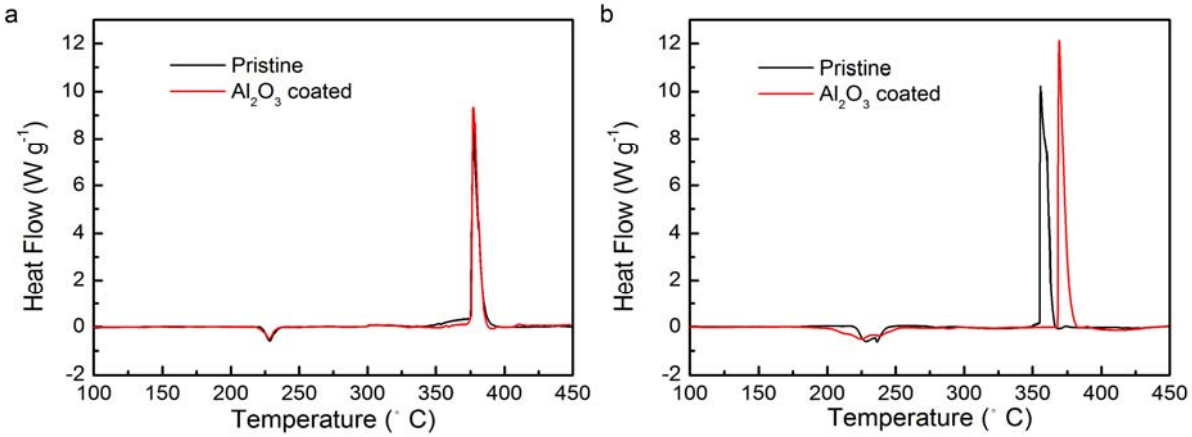

Fig. 8 DSC curves of the sealed pan with pristine or Al_2O_3 coated electrode material and electrolyte (a) 1st charged to 4.8 V and (b) Charged to 4.8 V after 20 cycles

Table 1 Comparison of initial charge-discharge capacities and coulombic efficiencies of pristine and coated electrodes

	Charge (mAh g^{-1})	Discharge (mAh g^{-1})	Coulombic efficiency
Pristine (2-4.8 V)	277.2	230.6	83.2%
Coated (2-4.8 V)	247.9	218.7	88.2%
Pristine (3-4.6 V)	275.2	225.0	81.8%
Coated (3-4.6 V)	236.8	199.4	84.2%

Table 2 Comparison of voltage drop before the beginning of each discharging

	2-4.8 V				3-4.6 V					
Cycle	1^{st}	10^{th}	20^{th}	30^{th}	1^{st}	20^{th}	40^{th}	60^{th}	80^{th}	100^{th}
Pristine	0.29	0.52	0.68	0.81	0.10	0.27	0.34	0.42	0.48	0.55
Coated	0.15	0.36	0.41	0.47	0.10	0.13	0.15	0.18	0.21	0.26

Table 3 Impedance parameters of equivalent circuits and cell potentials in EIS measurements

	Pristine				Al_2O_3 coated			
	R_s /Ω	R_{sei} /Ω	R_{ct} /Ω	Potential /V	R_s /Ω	R_{sei} /Ω	R_{ct} /Ω	Potential /V
(2-4.8 V) 20 cycles	0.27	8.2	219.4	3.66	0.23	14.1	60.8	3.65
(2-4.8 V) 50 cycles	0.35	6.2	308.1	3.71	0.87	10.5	129.6	3.68
(3-4.6 V) 50 cycles	1.1	7. 3	37.7	3.67	0.27	12.0	16.3	3.66
(3-4.6 V) 100 cycles	1.1	3.1	94.9	3.69	0.77	9.59	40.4	3.67